Hindawi
Complexity
Volume 2021, Article ID 6642706, 13 pages
https://doi.org/10.1155/2021/6642706

Research Article

Further Investigations on the Dynamics and Multistability Coexisted in a Memory-Based Cobweb Model

S. S. Askar [1,2]

[1] *Department of Statistics and Operations Research, College of Science, King Saud University, Riyadh 11451, Saudi Arabia*
[2] *Department of Mathematics, Faculty of Science, Mansoura University, Mansoura 35516, Egypt*

Correspondence should be addressed to S. S. Askar; s.e.a.askar@hotmail.co.uk

Received 14 December 2020; Revised 8 February 2021; Accepted 11 March 2021; Published 22 March 2021

Academic Editor: Pengfei Hu

Based on a nonlinear demand function and a market-clearing price, a cobweb model is introduced in this paper. A gradient mechanism that depends on the marginal profit is adopted to form the 1D discrete dynamic cobweb map. Analytical studies show that the map possesses four fixed points and only one attains the profit maximization. The stability/instability conditions for this fixed point are calculated and numerically studied. The numerical studies provide some insights about the cobweb map and confirm that this fixed point can be destabilized due to period-doubling bifurcation. The second part of the paper discusses the memory factor on the stabilization of the map's equilibrium point. A gradient mechanism that depends on the marginal profit in the past two time steps is adopted to incorporate memory in the model. Hence, a 2D discrete dynamic map is constructed. Through theoretical and numerical investigations, we show that the equilibrium point of the 2D map becomes unstable due to two types of bifurcations that are Neimark–Sacker and flip bifurcations. Furthermore, the influence of the speed of adjustment parameter on the map's equilibrium is analyzed via numerical experiments.

1. Introduction

Different disciplines such as biology, engineering, and economy are characterized by real-life models which possess complex dynamic behaviors and multistability criteria. Economists and mathematicians have reported these behaviors in economic models such as monopoly, duopoly, and oligopoly models. In that direction, many studies have reported that the equilibrium points of these models can be destabilized due to different types of bifurcations such as flip and Neimark–Sacker. Our contribution in this paper focuses on further investigating on complex dynamic characteristics of the cobweb model constructed based on the nonlinear demand function and gradient mechanism. We follow in our paper the nice discussions given in the seminal articles of Ezekiel [1] and Naimzada [2]. In [1], the effects of prices in the fluctuations of certain markets have been explained. Some important aspects on supply and market demand have been investigated in [1]. Ezekiel in [3] has claimed that the quantity of production must be set based on time so that firms' producers can review prices and hence a time lag has to be made between supply and demand.

The current paper follows up the hypothesis of Ezekiel and the discussion made by Naimzada in order to set up and analyze the suggested cobweb model. Building this model does not require assuming that the firms (or producers) have no full knowledge about market information but they have to have only knowledge about the demand. We adopt here an irrational function that is used to represent the demand. Using this kind of knowledge and the clearing price condition, the producer can update its production due to the variations that occurred in the marginal profit. Recalling the bounded rationality mechanism defined elsewhere [2], the producer may decrease or increase its outputs depending on the decrease or increase taking place in the marginal profit. In order to brief the outcomes of this paper, we divide the contribution into two important parts: the first part deals with the studies and investigations on a one-dimensional nonlinear discrete-time map describing the change in price. It has four nonzero real fixed points and only one of them attains the maximum value of the profit. The stability conditions of this point are calculated and some insights about it are provided based on analytical and numerical analysis. In the second part, we introduce the memory and convert the 1D map into a two-dimensional map. The 2D map contains two important parameters; the parameter of memory and the other for the adjustment speed. The memory parameter is represented by some weights that their influences on the stability of the equilibrium point are discussed. Through some analytical and numerical experiments, we show that low and high values for the memory parameter affect the stabilization of the equilibrium point due to the coexistence of Neimark–Sacker and period-doubling bifurcations. Based on the global analysis, some dynamic behaviors of the map such as multistability and chaotic attractors are reported. Some of those behaviors possess attractive basin with lobes from divergent points. Furthermore, we study the influence of the speed of adjustment by assuming equal memory weights. Some dynamic characteristics are obtained and discussed through pushing the global analysis towards the speed of adjustment parameter.

Both local and global analyses regarding bifurcation analysis and chaotic attractors within this paper have been carried out based on similar investigations and discussions. For instance, Shabbir et al. in [4] have introduced a new discrete-time system based on cannibalism in the prey population with the addition of Allee effects. They have calculated the system's fixed points and have discussed their stability that becomes unstable due to period-doubling and Neimark–Sacker bifurcation. In [5], the dynamic characteristics such as topological classification, Lyapunov exponents, and manifold theory have been investigated for the Goodwin model. Din and Haider in [6] have studied the complex dynamic characteristics of the discrete-time version of the Schnakenberg model. In [7], a deterministic oligopoly model whose players are heterogeneous has been introduced and its dynamic behaviors that are formed based on best responders and imitators have been discussed. Agliari et al. in [8] have given an intensive dynamic analysis for a Cournot duopoly game with differentiated goods whose players are homogenous and have adopted a gradient-based mechanism in order to update their outputs. Other interesting studies that have adopted discrete dynamic systems and their complex dynamic characteristics in different applications such as engineering have been reported in Bao et al. [9], Li et al. [10], and Bao et al. [11].

Briefly, the paper consists of six sections. The first section introduces the main contribution of the paper. In Section 2, the literature review is reported. In Section 3, the 1D cobweb map is given and studied. The influence of memory is investigated in Section 4. The influence of the speed of adjustment is analyzed in Section 5. Finally, we conclude the obtained results in Section 6.

2. Literature Review

Several economic contexts have reported in literature different studies and investigations on the cobweb model. We highlight in this section some of those studies. For example, different sectors in the economic market have reported the cobweb model where there are academia [2], real estate [12], nurses [13], potatoes [14], and bioenergy crops [15]. Based on nonlinear demand and supply functions the equilibrium points of cobweb mode have been calculated and their stability conditions have been investigated in [16]. In [17], the adaptive expectation was used to form complex cobweb models. In [18], the traditional cobweb model has been constructed using a nonlinear supply function and it has been reported that period-doubling cycles can be found when firms adopt the adaptive expectation mechanism. In [19], the authors have detected chaotic behaviors for a standard cobweb model whose players adopted adaptive expectations using monotonic demand and supply functions. Based on linear demand and nonlinear supply functions, the dynamics of the cobweb map have been investigated under adaptive expectations in [20].

The studies mentioned above have proposed certain assumptions about the producers (or firms). They have assumed that those producers possessed somehow the cost function and hence they can calculate the profit which depends on produced quantity and its price. Indeed, this gives producers some knowledge on the determination of quantities sent to the economic market as price-based functions. Such hypotheses have given rise to many mechanisms such as the bounded rationality mechanism to model the dynamic economic behaviors behind these hypotheses. For example, a cobweb model has been constructed and described by a nonlinear discrete dynamical system using a gradient mechanism in [2]. The authors in this study assumed that producers have no complete knowledge of demand and they instead perform empirical estimations on marginal profit. The bounded rationality approach is an effective mechanism adopted when dealing with such economic systems and information about it has been reported elsewhere in the literature ([3, 21–30]). Furthermore, the bounded rationality has been adopted in many studies in the literature that require knowledge and computational experiments. For instance, in [31], a cobweb model whose supply and demand are nonlinear functions has been investigated. In that study, the producers have recalled the mechanism of backward expectation to make prices forecasting in the future evolution. This mechanism adopted in [31] depended on prices given in the last two periods. In [32], another mechanism that is called naive expectation has been used by producers with more general demand and cost functions in a cobweb model. Other studies in the literature have suggested rational producers in [33], heterogeneous producers in [34], and replicator dynamics in [35].

3. The Cobweb Model

Let $D(p)$ be the consumer demand, where p refers to price. This demand function may be linear or nonlinear depending on the preferences of the consumer. In this paper, we consider throughout this paper the following nonlinear demand:

$$q_D(t) = D(p(t)) = a - \sqrt{p(t)}, \quad a > 0, \; p(t) > 0, \tag{1}$$

where t represents the time. It is clear that $q_D(t) = 0$ means the market is not supported by quantities and then the consumer is willing to buy a unit of production with a maximum price that is a^2. From (1) we get

$$p(t) = D^{-1}(q_D(t)) = (a - q_D(t))^2, \tag{2}$$

that represents the inverse of demand. In order to provide the market with produced quantities at time $t+1$, producers make the estimation of some factors raised at time t. Of these factors are the production volume and gained profit. They receive lack of market information and then perform market experiments so that they can decide the market state. Based on these factors, producers decide to supply the market with quantities demanded. They increase the amount of production in the next period of time if the profit increases and they reduce the amount if the profit is decreased. The profit of quantity supplied to the market may be given by

$$\pi(q_S(t)) = p(t) q_S(t) - \mathrm{TC}(q_S(t)), \tag{3}$$

where $q_S(t) \geq 0$ represents supplied quantity at time t and $\mathrm{TC}(q_S(t))$ denotes the total cost. This total cost is taken as a linear function as follows:

$$\mathrm{TC}(q_S(t)) = c q_S(t), \tag{4}$$

where c is the marginal cost $(c = (\mathrm{dTC}/\mathrm{d}q_S) > 0)$. The cobweb theory states that attaining market equilibrium can be obtained by assuming $q_D(t) = q_S(t) = q(t)$ at any time t. Therefore, (3) can be rewritten as follows:

$$\pi(q(t)) = q(t)[a - q_D(t)]^2 - c q(t). \tag{5}$$

From (5), one gets a positive profit if $a > \sqrt{c}$. This indicates that the maximum price a^2 paid for buying a unit of commodity must be greater than the value c. On the other hand, if $a < \sqrt{c}$, the profit becomes negative that has no economic meaning. Differentiating (5) gives the following marginal profit:

$$\psi(q(t)) = \frac{\mathrm{d}\pi(q(t))}{\mathrm{d}q(t)} = (a - q(t))^2 - 2q(t)(a - q(t)) - c. \tag{6}$$

Now, the quantity supplied to the market at $t+1$ can be stated as follows:

$$\begin{aligned} q_S(t+1) &= q(t) + k(q(t))\psi(q(t)) \\ &= q(t) + k\left((a - q(t))^2 - 2q(t)(a - q(t)) - c\right), \end{aligned} \tag{7}$$

where we take $k(q(t)) = k$ as a positive parameter known as the speed of adjustment. Using (1) in (7), one can simplify the supply in the form

$$\begin{aligned} q_S(t+1) = S(p(t)) = a - \sqrt{p(t)} \\ + k[\sqrt{p(t)}(3\sqrt{p(t)} - 2a) - c], \end{aligned} \tag{8}$$

and then market-clearing price gives

$$q_D(t+1) = q_S(t+1). \tag{9}$$

From (1) and (8), we get

$$a - \sqrt{p(t+1)} = a - \sqrt{p(t)} + k[\sqrt{p(t)}(3\sqrt{p(t)} - 2a) - c]. \tag{10}$$

After some simple calculations, the price at time $t+1$ can be expressed by the following one-dimensional discrete dynamic map:

$$p(t+1) = f(p(t)) = (\sqrt{p(t)} - k[\sqrt{p(t)}(3\sqrt{p(t)} - 2a) - c])^2. \tag{11}$$

It possesses four fixed points given by

$$\begin{aligned} \overline{p}_1 &= \frac{1}{3}\left[c + \frac{2a}{3}\left(a + \sqrt{a^2 + 3c}\right)\right], \\ \overline{p}_2 &= \frac{1}{3}\left[c + \frac{2a}{3}\left(a - \sqrt{a^2 + 3c}\right)\right], \\ \overline{p}_3 &= \frac{1}{9k^2}\left[2 + 4ak + 3ck^2 + 2a^2k^2 + (2 + ak)\sqrt{1 + 2ak + 3ck^2 + a^2k^2}\right], \\ \overline{p}_4 &= \frac{1}{9k^2}\left[2 + 4ak + 3ck^2 + 2a^2k^2 - (2 + ak)\sqrt{1 + 2ak + 3ck^2 + a^2k^2}\right]. \end{aligned} \tag{12}$$

Since the parameters a, c, and k are positive, then both $\overline{p}_1$ and $\overline{p}_3$ are positive. The other two points are positive under certain conditions. Before we discuss the stability conditions for these fixed points and detect their complex dynamic behaviors, we investigate the relation between the demand and supply depicted in Figures 1(a) and 1(b). One can see that both q_D and q_S intersect in the equilibrium price $\overline{p}_1$. It must not exceed the maximum price a^2 that is guaranteed

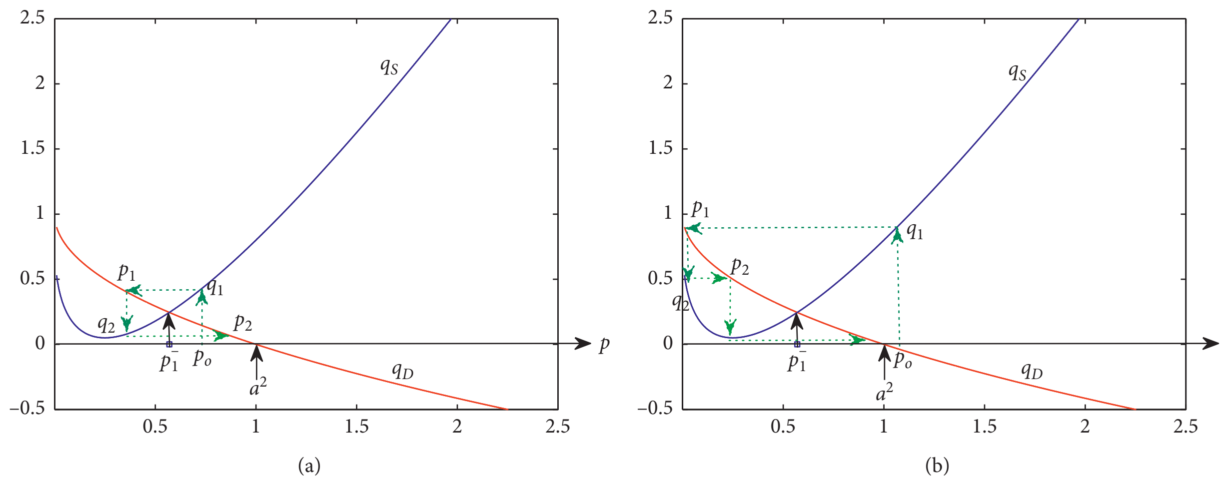

FIGURE 1: Dynamic steps for price and quantity for different initials of price. Parameters' values are $a = 1, c = 0.2, k = 1$.

based on the condition $a^2 > c$; otherwise, a negative price may be raised if $a^2 < c$. Starting at p_o while $0 < p_o < a^2$ and moving vertically until reaching q_S which is represented by the blue curve, we get the quantity in the next period that is denoted by q_1 in Figure 1(a). Since our model is in an equilibrium state at each period of time, we have equal demand and supply and consequently, we move horizontally to q_D (represented by the red curve in Figure 1(a)) to get the price p_1 that is being used to set q_2 in the next period. After setting q_2, we move horizontally to p_2 (represented by the red curve in Figure 1(a)). This procedure is repeated till reaching the equilibrium of market price $\overline{p}_1$. Figure 1(b) shows this procedure for an initial price $p_o > a^2$. From this discussion, we conclude that the trajectories of cobweb will not approach negative values.

Now, we begin discussing the dynamics of map (11) around the fixed points which depend on the parameters a and c. The profit represented by (5) can be rewritten as follows:

$$\pi(p) = (p - c)\left(a - \sqrt{p(t)}\right) \tag{13}$$

Differentiating (13), we get $(d\pi/dp)|_{p=\overline{p}_1,\overline{p}_2} = 0$ but the profit attains its maximum value at the equilibrium price $\overline{p}_1$. Furthermore, we have $\pi(c) = 0$ and $\pi(p) > 0$ if $c < p < a^2$. This means that when we increase the price p in the interval $(c, \overline{p}_1]$, the profit variations become positive while they get negative for $\overline{p}_1 < p < a^2$. This may be explained due to the monotonic or nonmonotonic way of the production level carried out by producers and the way they deal with the change in profit. Figure 2 confirms that the marginal profit intersects the abscissa axis exactly in $\overline{p}_1$ (the market equilibrium price).

Proposition 1. *The stability/instability of market equilibrium price $\overline{p}_1$ is constrained by the following possibilities:*

(i) The equilibrium price is locally stable if $(1/2\Phi) < k < (1/\Phi)$

(ii) The equilibrium price is unstable if $k > (1/\Phi)$

where

$$\Phi = \sqrt{2a\sqrt{a^2 + 3c} + 3c + 2a^2} - a. \tag{14}$$

Proof. Recalling the marginal demand and marginal supply at $\overline{p}_1$ gives

$$\frac{S'(\overline{p}_1)}{D'(\overline{p})} = 1 + 2k\left(a - \sqrt{2a\sqrt{a^2 + 3c} + 3c + 2a^2}\right) \tag{15}$$

Using the conditions given in [36], we get

(i) The equilibrium price is locally stable if $-1 < (S'(\overline{p})/D'(\overline{p})) < 0$

(ii) The equilibrium price is unstable if $(S'(\overline{p})/D'(\overline{p})) < -1$

So, the proof is completed after substituting (15) in the above conditions.

Now, we study the influences of the parameters a, c, and k on the dynamics of the map. We perform some numerical experiments to investigate more these dynamics. The influence of the speed of adjustment parameter k while fixing the other parameters is given in Figure 3(a). We assume the following parameters' values $a = 1, c = 0.2, 0.5$. Figure 3(a) shows two situations: the first one presents the period-doubling diagram with respect to k at $a = 1$ and $c = 0.2$. It shows that the equilibrium point becomes locally stable; then, it becomes unstable. For this situation, several numerical experiments have been carried out using low marginal cost and we have concluded that such low marginal cost guarantees stable situation for the equilibrium price. On the other hand and as shown in Figure 3(b), the increase in marginal cost causes a reduction in the region of stability for the equilibrium price. It would be a stability region as long as the condition $a^2 > c$ that preserves nonnegative price and stability of the equilibrium market price too. For the parameters a and c, we fix the speed of adjustment parameter k and study the impact of a and c. As given in Figure 3(b), the

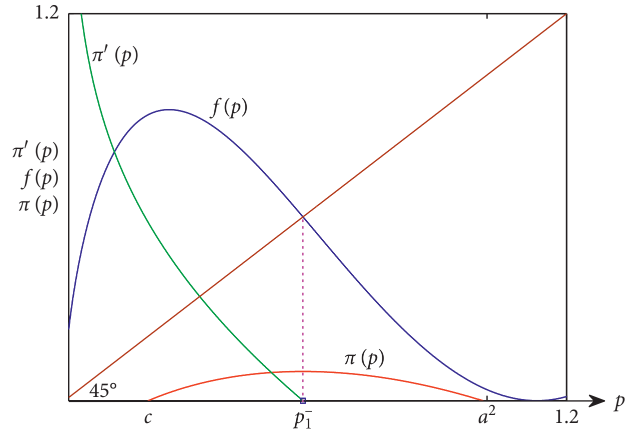

Figure 2: The shapes of the functions $\pi'(p)$, $f(b)$, and $\pi(p)$ along with a line with 45°. It is obvious that $\pi(c)$ and $\pi(a^2)$ are vanished while $\max \pi(p)$ is obtained at $\bar{p}_1$. The other parameters' values are $a = 1, b = 0.2, k = 1$.

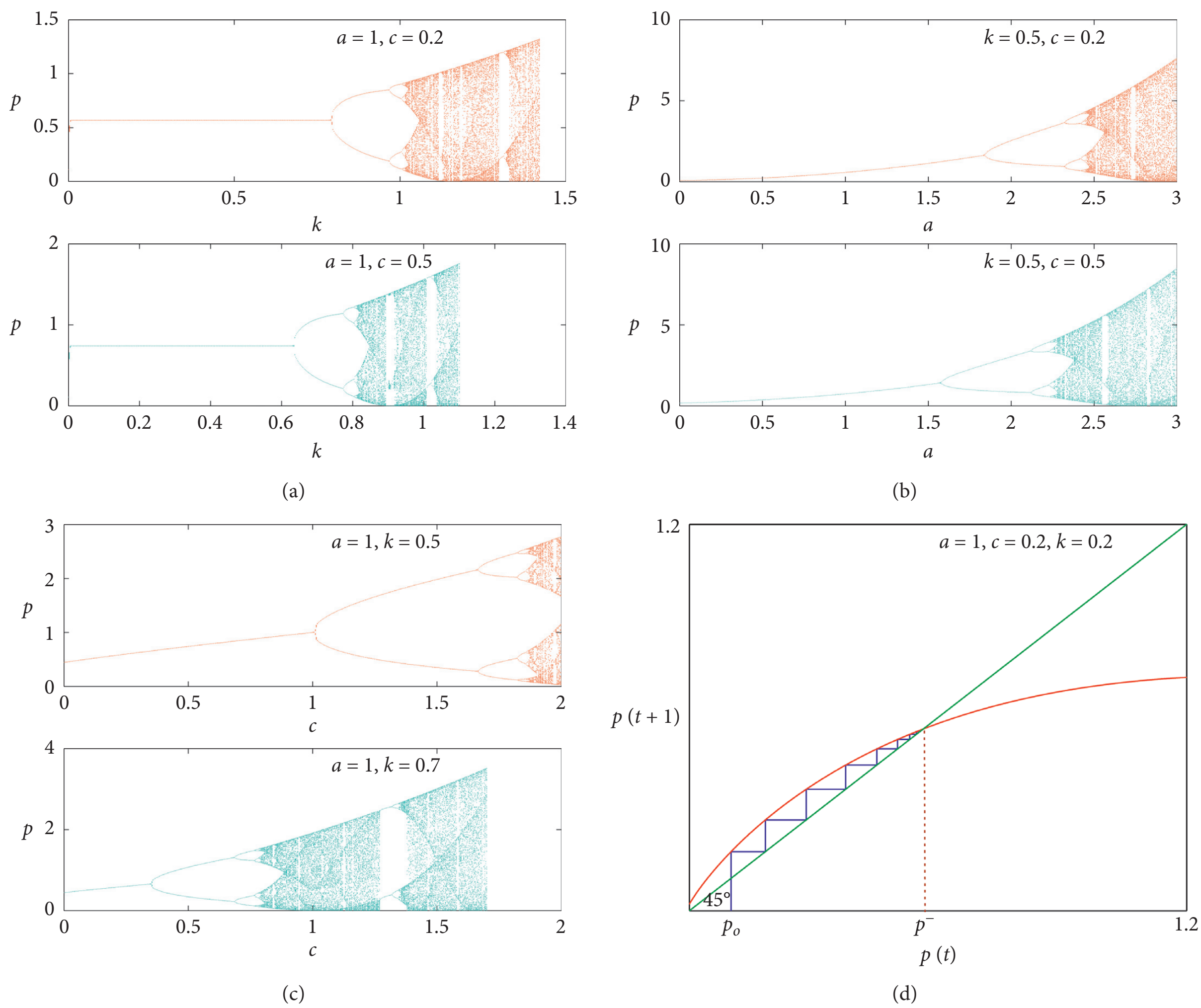

Figure 3: Continued.

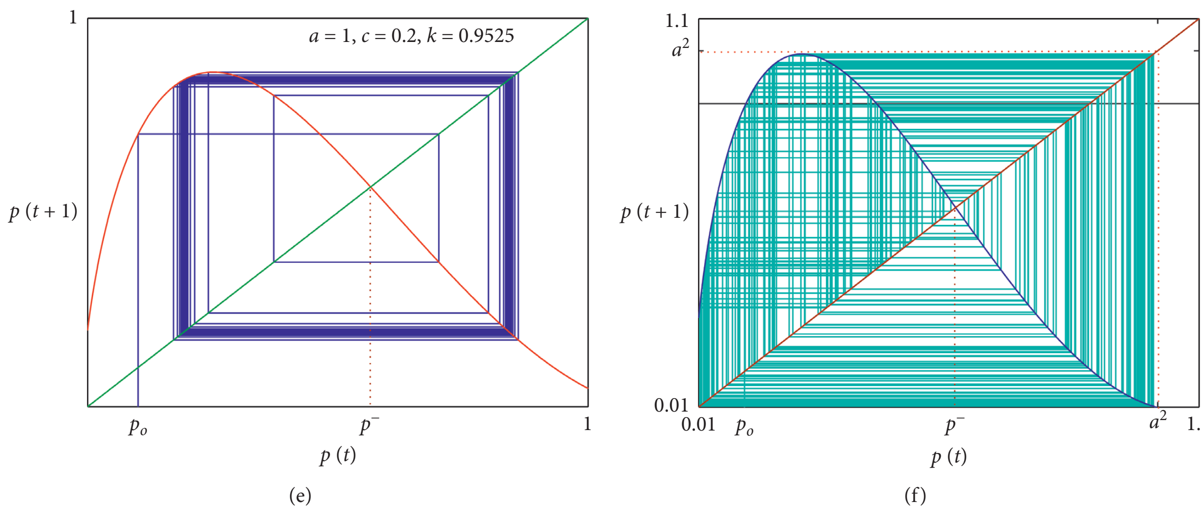

Figure 3: Bifurcation shape of p versus (a) k at $a = 1, c = 0.2, 0.5$, (b) a at $k = 0.5, c = 0.2, 0.5$, and (c) c at $a = 1, k = 0.5, 0.7$. Basins of attraction of different attracting set for the map (11) at the parameters set: (d) $k = 0.2$, (e) $k = 0.9525$, and (f) $k = 1.11$. Other parameters' values are $a = 1, c = 0.2$.

parameter a affects the stability of the equilibrium point and makes it loses its stability via period-doubling bifurcation for low and high marginal cost. The same discussion is given for the parameter c as depicted in Figure 3(c). These numerical experiments confirm the impact of the map's parameters on the local stability of the equilibrium price. This urges us to investigate more some of the global investigation of the dynamics of the map. We begin with the set of parameters values, $k = 0.2, a = 1, c = 0.2$. Figure 3(d) shows that there is a monotonic convergence to the equilibrium market price $\overline{p}_1$. Further increase in the parameter k to the value 0.9525 gives rise to a sequence of period-doubling whose attractive basin is given in Figure 3(e). As k increases further and the other parameters are fixed, higher cycles are obtained until $k = 1.11$ where a chaotic behavior of the map is born in Figure 3(f). Other numerical experiments have been carried out for different values of k and have shown that the attracting set of any period cycles or chaotic behavior will have an attractive basin that is bounded within the box $[0, a^2] \times [0, a^2]$. Therefore, any initial prices that are chosen out of this box will lead to negative or unbounded trajectories that have no meaning in economy. □

4. Memory Effect on the Cobweb Model (2D Map)

This section introduces the memory in the map (11). The memory here means that producers decide whether they increase or decrease the production in the next period of time. It is given by [37]

$$q_S(t+1) = q(t) + k\left[\omega \frac{\partial \pi(q(t))}{\partial q(t)} + (1-\omega)\frac{\partial \pi(q(t-1))}{\partial q(t-1)}\right], \quad \omega \in [0,1] \tag{16}$$

This memory is estimated by producers based on the marginal profits at two periods, the previous period $t-1$ and the current period t with weight ω in order to provide the market with the supplied quantity at $t+1$. Using (6), we get

$$\begin{aligned} q_S(t+1) = a - \sqrt{p(t)} + k[\omega(\sqrt{p(t)}\,(3\sqrt{p(t)} - 2a) - c) \\ + (1-\omega)(\sqrt{p(t-1)}\,(3\sqrt{p(t-1)} - 2a) - c)] \end{aligned} \tag{17}$$

Imposing the market clearing $q_S(t+1) = q_D(t+1)$ gives

$$p(t+1) = (\sqrt{p(t)} - k[\omega(\sqrt{p(t)}\,(3\sqrt{p(t)} - 2a) - c) + (1-\omega)(\sqrt{p(t-1)}\,(3\sqrt{p(t-1)} - 2a) - c)])^2. \tag{18}$$

Setting $p(t) = x_t$ and $p(t-1) = y_t$ in (18), a two-dimensional (2D) map is obtained:

$$T: \begin{cases} x_{t+1} = \left(\sqrt{x_t} - k\left[\omega\left(\sqrt{x_t}\left(3\sqrt{x_t} - 2a\right) - c\right) + (1-\omega)\left(\sqrt{y_t}\left(3\sqrt{y_t} - 2a\right) - c\right)\right]\right)^2, \\ y_{t+1} = x_t. \end{cases} \quad (19)$$

For the map (19), we get four fixed points and we focus only on the one in the form $O = (\overline{p}_1, \overline{p}_1)$ where $\overline{p}_1$ is given by (11). The following propositions are used in discussing the stability/instability conditions of this point.

Proposition 2. *Suppose that λ_1 and λ_2 are two eigenvalues for the Jacobian matrix of (19) at O; then,*

(i) O is an attracting node and is locally stable if $|\lambda_{1,2}| < 1$.

(ii) O is repelling node and unstable if $|\lambda_{1,2}| > 1$.

(iii) O is a saddle point and is unstable if $|\lambda_1| < 1$ and $|\lambda_2| > 1$ (or $|\lambda_1| > 1$ and $|\lambda_2| < 1$).

(iv) O is a nonhyperbolic point if $|\lambda_1| = 1$ and $|\lambda_2| \neq 1$ (or $|\lambda_1| \neq 1$ and $|\lambda_2| = 1$).

Proposition 3. *The point O is local stable if the following conditions are satisfied:*

$$\begin{aligned} 1 - \left[1 + 2k\left(a - 3\sqrt{\overline{p}_1}\right)\right]\left(1 + 2ak + \frac{ck}{\sqrt{\overline{p}_1}} - 3k\sqrt{\overline{p}_1}\right) &> 0, \\ 1 + \left[1 - 2k(1-2\omega)\left(a - 3\sqrt{\overline{p}_1}\right)\right]\left(1 + 2ak + \frac{ck}{\sqrt{\overline{p}_1}} - 3k\sqrt{\overline{p}_1}\right) &> 0, \\ 1 + 2k(1-\omega)\left(a - 3\sqrt{\overline{p}_1}\right)\left(1 + 2ak + \frac{ck}{\sqrt{\overline{p}_1}} - 3k\sqrt{\overline{p}_1}\right) &> 0. \end{aligned} \quad (20)$$

Proof. Proof. We recall Jury conditions [38] that are given by

$$\begin{aligned} g(1) &:= 1 - \tau + \delta > 0, \\ g(-1) &:= 1 + \tau + \delta > 0, \\ \Delta &:= 1 - \delta > 0, \end{aligned} \quad (21)$$

where τ and δ represent trace and determinant of the Jacobian matrix of the map (19) at O and are given by

$$\begin{aligned} \tau &= \left(1 + 2ak\omega - 6k\omega\sqrt{\overline{p}_1}\right)\left(1 + 2ak + \frac{ck}{\sqrt{\overline{p}_1}} - 3k\sqrt{\overline{p}_1}\right) \\ \delta &= 2k(1-\omega)\left(3\sqrt{\overline{p}_1} - a\right)\left(1 + 2ak + \frac{ck}{\sqrt{\overline{p}_1}} - 3k\sqrt{\overline{p}_1}\right) \end{aligned} \quad (22)$$

We should highlight here the types of bifurcations that may have occurred based on these conditions. If $g(1) = 0$ while $g(-1) > 0$ and $\Delta > 0$, then O becomes unstable due to transcritical or fold bifurcation. If $g(-1) = 0$ while $g(1) > 0$ and $\Delta > 0$, then O becomes unstable due to period-doubling bifurcation. But if $\Delta = 0$ and $g(1) > 0$ and $g(-1) > 0$, then O can be destabilized due to Neimark–Sacker bifurcation ([8, 29]). Substituting (22) in (21) completes the proof.

Hence, the conditions in (20) are used to detect the conditions of stability/instability of O. Because of the complicated form of the equilibrium point O, some numerical simulations are performed in order to get more insights about the conditions given in (20). It is clear that both $g(-1)$ and Δ contain the parameter ω that represents the memory. Therefore, we analyze the effects of ω on the stability of the equilibrium point O. We begin with the set $a = 1.4, c = 0.55, k = 0.68$, and $\omega = 0.62$. It gives $O = (1.21, 1.21)$ and then the Jacobian becomes

$$J_O \approx \begin{pmatrix} -0.60210 & -0.98192 \\ 1 & 0 \end{pmatrix}. \quad (23)$$

For J_O, we get two complex conjugate eigenvalues, $\lambda_{1,2} = -0.30104 \pm 0.94408i$ with $|\lambda_{1,2}| \approx 0.99092 < 1$, and hence O is locally stable point. Furthermore, we have $\tau = -0.60210$ and $\delta = 0.98192$ and hence $\delta < 1$ means that the map (19) is dissipative. It is easy to see that the conditions in (20) are all satisfied and then O is locally asymptotically stable. In Figure 4(a), we depict how the parameter ω affects the equilibrium point O. It shows the bifurcation diagram and that there are two types of bifurcations found between ω and the variable x. The assumed set of parameters' values shows that the equilibrium point O becomes unstable because of the coexisting of Neimark–Sacker bifurcation for values ω in the interval $0 \le \omega \le \omega_{ns}$ while, in the interval $\omega \in [\omega_f, 1]$, the equilibrium point becomes unstable due to flip bifurcation. Now, we perform some numerical experiments in order to

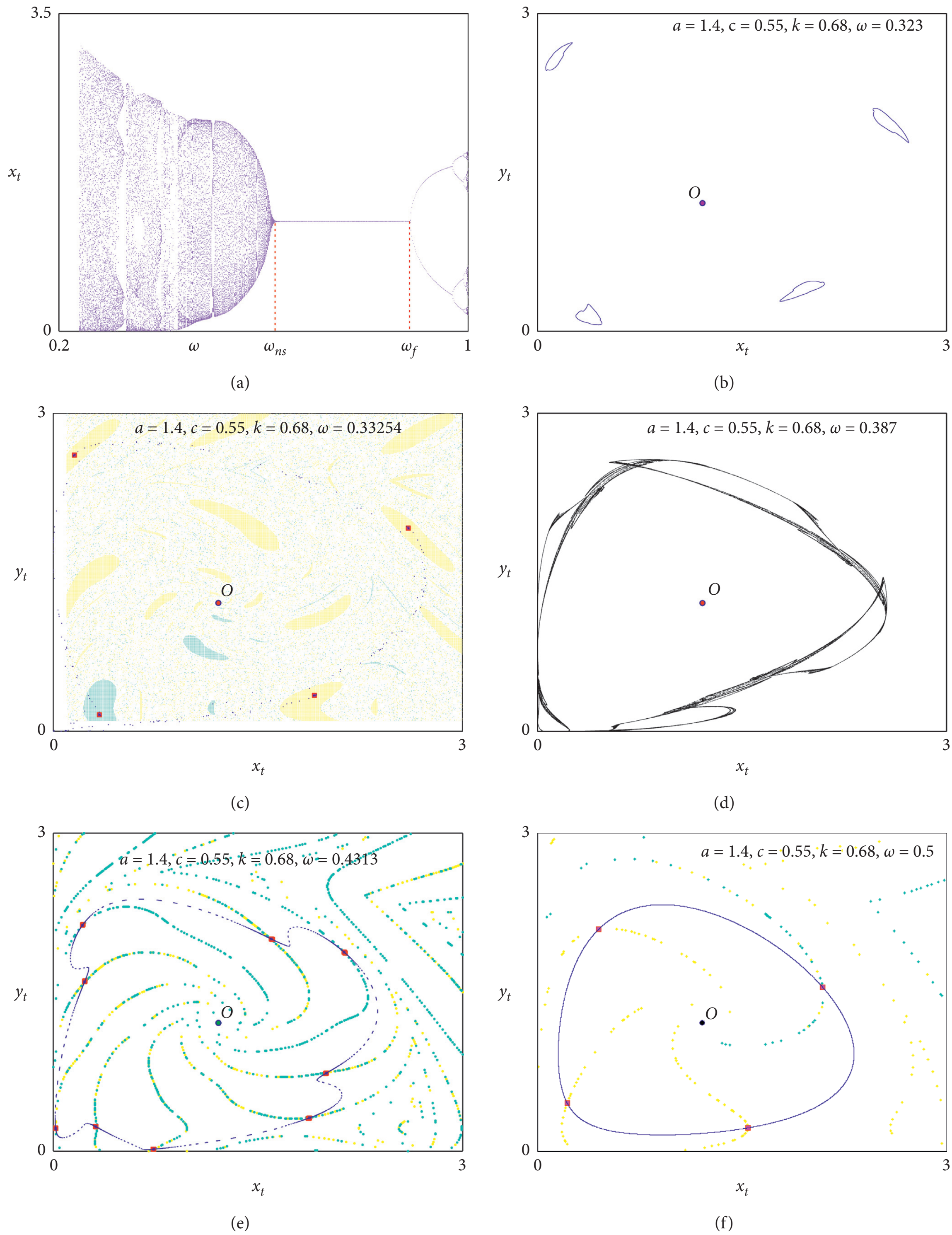

FIGURE 4: Continued.

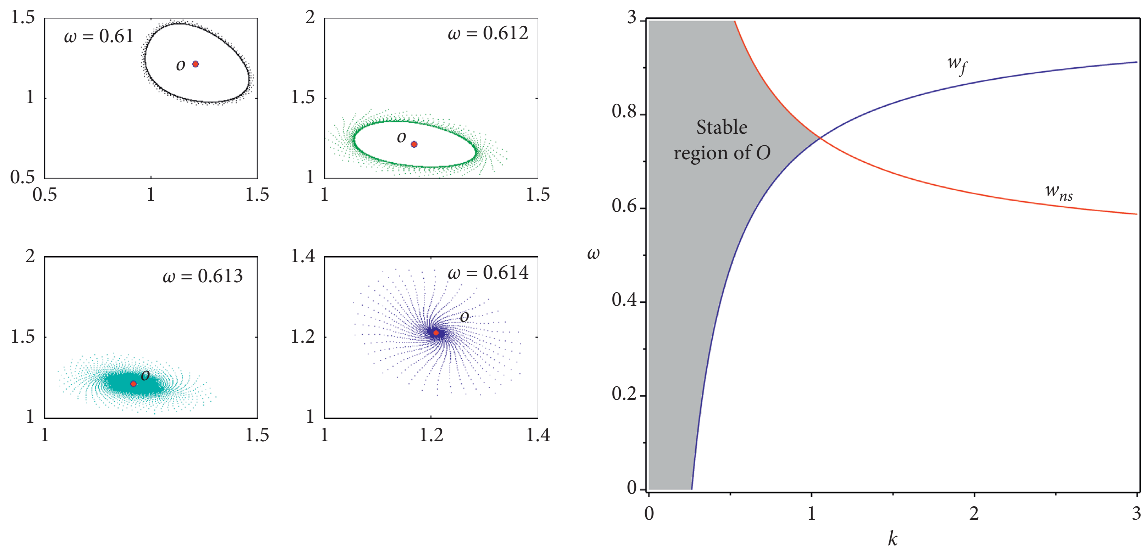

(g) (h)

Figure 4: (a) Bifurcation diagram of ω at $k = 1.4$. (b) Phase plane for four disconnected closed rings at $\omega = 0.323$ and $k = 0.68$. (c) The attractive basins of period-4 cycle and chaotic attractor at $\omega = 0.33254$ and $k = 0.68$. (d) The phase plane of strange attractor around O at $\omega = 0.387$ and $k = 0.68$. (e) The attractive basins of period-9 cycle with chaotic attractor at $\omega = 0.4313$ and $k = 0.68$. (f) The attractive basins of period-4 cycle with a closed invariant curve at $\omega = 0.5$ and $k = 0.68$. (g) Different dynamic behaviors at $\omega = 0.6.1, 0.612, 0.613, 0.614$ and $k = 1.4$. (h) The stability region and chaos routes via the Neimark–Sacker and flip bifurcations. The other values of parameters are $a = 1.4$ and $c = 0.55$.

investigate more the global dynamic behavior of the map (19) around O. Keeping the parameters' values fixed and changing ω to 0.323, the dynamics of the map around the equilibrium are converted into four closed rings. The phase portrait for those closed rings is given in Figure 4(b). Increasing ω to 0.33254 gives rise to a period-4 cycle (denoted by squares) with a disconnected chaotic attractor (red) around the unstable equilibrium O for the same set used for the bifurcation diagram. It is plotted in Figure 4(c) with its basins of attraction that it consists of two colors: yellow and cyan. A further increase in the memory parameter to $\omega = 0.387$ makes the map becomes more chaotic and we get a chaotic behavior around O as shown in Figure 4(d). At $\omega = 0.4313$, the attractive basins of period-9 cycle (denoted by squares) together with the basin of a closed chaotic attractor (red) that surrounds the unstable O are displayed in Figure 4(d). This period-9 cycle (as shown in Figure 4(e)) disappears when we increase ω to 0.5. At $\omega = 0.5$, we get a period-4 cycle together with a closed invariant curve surrounding the point O. This dynamic situation is given in Figure 4(f) where the yellow and cyan colors refer to the attractive basins of the period-4 cycle. For further increase in ω, the previous dynamic situation is disappeared and we get instead a spiral point. We give in Figure 4(g) different dynamic behaviors for the map at $\omega = 0.61, 0.612, 0.613$ and $\omega = 0.614$. In Figure 4(h), we depict the stability region for the point O at the parameters set, $a = 1.4, c = 0.55$ in the $(k, \omega)-$plane. It is clear that when $\omega = 0$ and $k \geq 0.2631578947$, the point O becomes unstable via the Neimark–Sacker bifurcation as k increases. As ω becomes close to a uniform distribution, the stability region of O is extended as k increases. For values of ω above 0.75, this stability region of O is reduced with respect to k and then O becomes unstable through flip bifurcation. This investigation makes us analyze in the $(k, \omega)-$plane the 2D bifurcation diagram. This bifurcation diagram is given in Figure 5 at the set of parameters values, $a = 1.44$ and $c = 0.55$. We give at the end of this section a dynamic situation of chaotic attractor that is formed by four disconnected bands around O for a value of ω near to 1 as shown in Figure 6. □

5. The Speed of Adjustment and Its Effect

We assume $\omega = (1/2)$ that represents a symmetric case in the map (19) as follows:

$$T: \begin{cases} x_{t+1} = \left(\sqrt{x_t} - k\left[0.5\left(\sqrt{x_t}\left(3\sqrt{x_t} - 2a\right) - c\right) + 0.5\left(\sqrt{y_t}\left(3\sqrt{y_t} - 2a\right) - c\right)\right]\right)^2, \\ y_{t+1} = x_t. \end{cases} \quad (24)$$

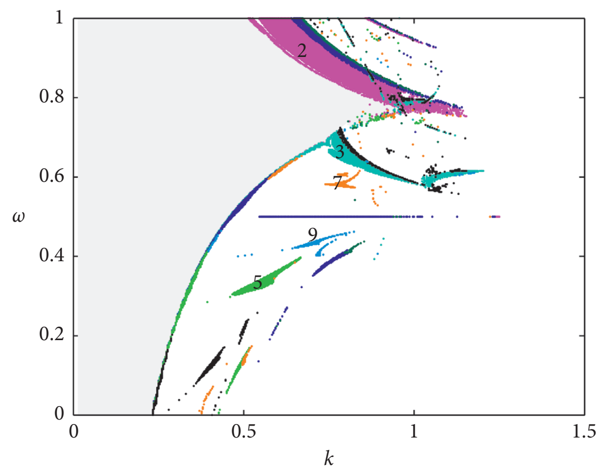

Figure 5: The 2D bifurcation diagram in the (k, ω) − plane. Different types of periodic cycles are numbered with different colors. The other parameters are $a = 1.4$ and $c = 0.55$.

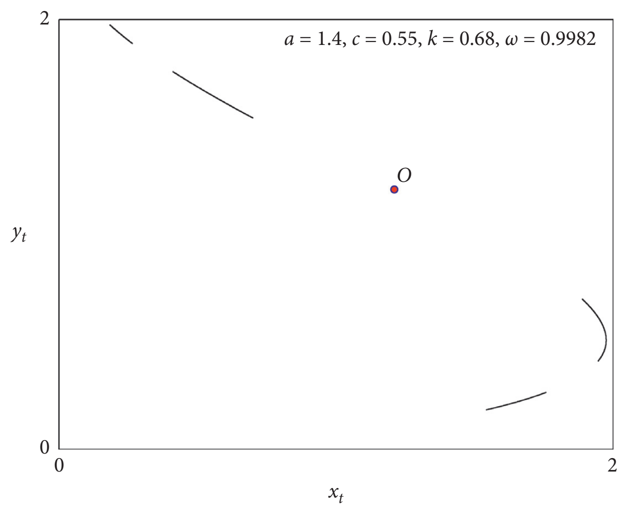

Figure 6: The phase plane of a chaotic attractor consisting of four bands at the parameters' values, $a = 1.4, c = 0.55, k = 0.68$, and $\omega = 0.9982$.

It means that producers adopt the average in marginal profits at the time steps $t-1$ and t. Now, the map (24) contains the parameters a, k, and c and we study in this section the effect of k on the dynamics of the map. Assuming $a = 0.4$ and $c = 0.11$, Figure 7(a) shows the 1D bifurcation diagram when varying the bifurcation parameter k. It shows that the equilibrium point O becomes stable for the values of k until k approaches the value 1.353 where the point O becomes unstable due to the Neimark–Sacker bifurcation. Increasing k to 1.423, the equilibrium point O converts into an unstable spiral point as shown in Figure 7(b). A further increase in k to 1.58 gives rise to a period-4 cycle. The basins of attraction of this cycle consist of yellow and cyan colors (as shown in Figure 7(c)) while the white color refers to the nonconvergent points. This cycle occurs as k increases until $k = 2.18$ where this cycle is converted into a chaotic attractor consisting of four disconnected bands (see Figure 7(d)). At $k = 2.36$, a period-5 cycle is born which has attractive basins with yellow and cyan colors. The dark gray refers to divergent points as given in Figure 7(e). After that, the dynamic of the map becomes chaotic for any increase in the parameter k. Figure 7(f) gives an example of the chaotic situation when $k = 2.76$. Regarding the parameters a and c numerical experiments show that increasing both parameters affect the stability region of O with respect to k.

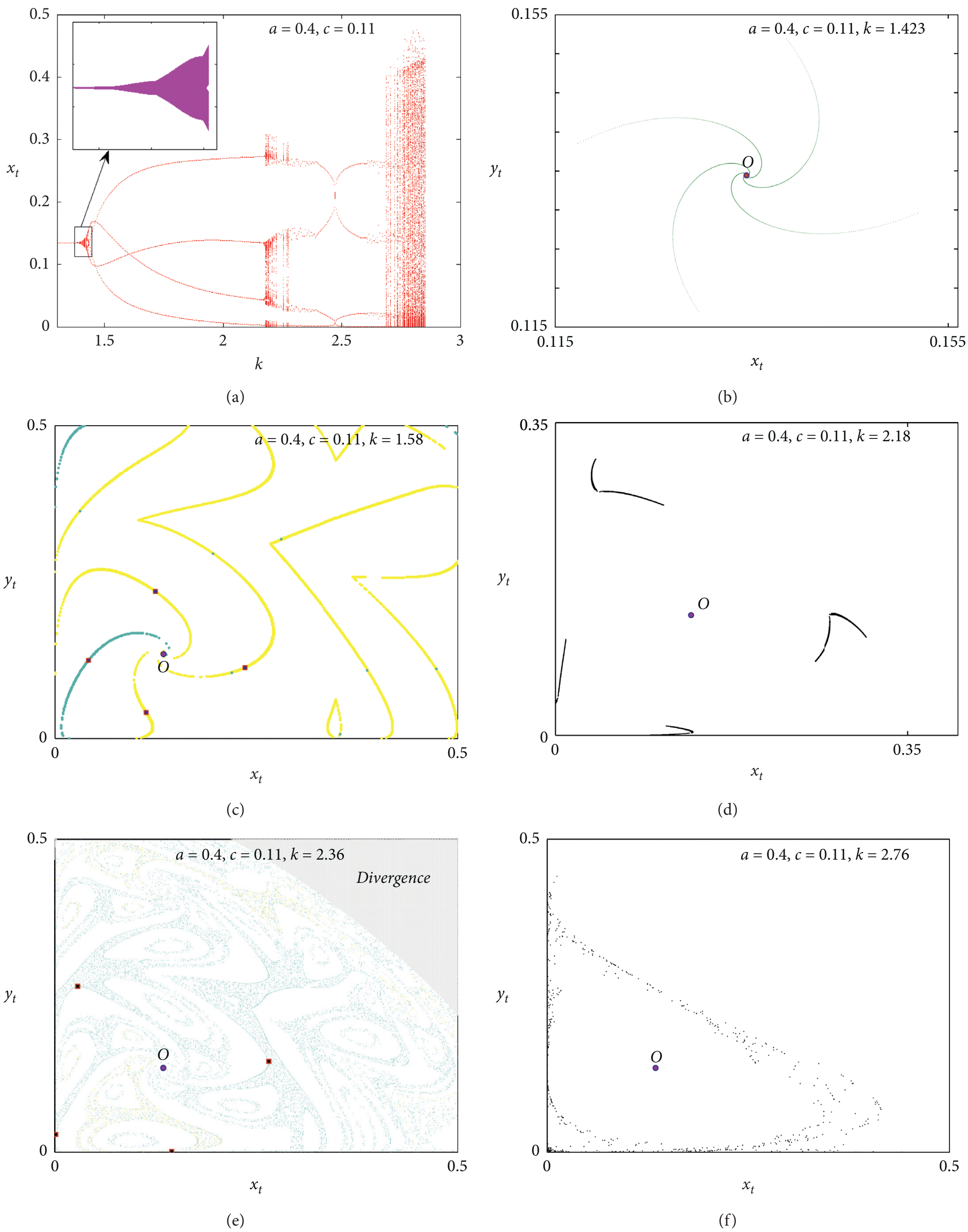

Figure 7: (a) The bifurcation diagram with respect to k at $a = 0.4, c = 0.11$. Different attracting sets. (b) A spiral at $a = 0.4, c = 0.11$, and $k = 1.423$. (c) Period-5 cycle at $a = 0.4, c = 0.11$, and $k = 1.58$. (d) Chaotic attractor at $a = 0.4, c = 0.11$, and $k = 2.18$. (e) Period-5 cycle at $a = 0.4, c = 0.11$, and $k = 2.36$. (f) Chaotic attractor at $a = 0.4, c = 0.11$, and $k = 2.76$.

6. Conclusion

In this work, we have investigated a cobweb model whose producers do not possess complete knowledge about the market and update their outputs according to the mechanism of bounded rationality. The producers have estimated their marginal profit by observing profit variations that might have occurred at the beginning of production. In the first part of this paper, we have studied the complex and chaotic behaviors of a one-dimensional discrete cobweb model. Our obtained results have shown that any increase in marginal cost leads to an unstable equilibrium price. Furthermore, we have shown that the equilibrium price for the 1D map becomes locally stable when the adjustment speed parameter takes low values. Higher values of that parameter have given rise to unstable price and therefore periodic cycles or chaotic attractors for the dynamics of price have coexisted.

The second part of this paper contains other contributions that are the inclusion of memory in the 1D model and converting it into a 2D discrete dynamic model. Based on a convex combination of marginal profit at the past two periods, the memory parameter has been incorporated ([31, 37]). Our investigations have analyzed the influence of the memory parameter on the equilibrium price and found that it has a qualitative effect on its stability. Using both analytical and numerical analysis we have discussed the stability/instability conditions of the equilibrium price. We have found that the equilibrium price may be unstable through period-doubling and Neimark–Sacker bifurcations when the memory parameter is used as the bifurcation parameter. Through simulation, we have reported multistability situations. Furthermore, the qualitative impact of the adjustment parameter has been analyzed in a symmetric case on which the average change in marginal profits has been considered.

Data Availability

The data sets generated during the current study are available from the corresponding author on reasonable request.

Conflicts of Interest

The authors declare that there are no conflicts of interest regarding this article.

Acknowledgments

The authors are grateful to the Research Supporting Project number (RSP-2020/167), King Saud University, Riyadh, Saudi Arabia. This project is funded by Saud University, Riyadh, Saudi Arabia.

References

[1] M. Ezekiel, "The cobweb theorem," *The Quarterly Journal of Economics*, vol. 52, no. 2, pp. 255–280, 1938.

[2] A. Naimzada and N. Pecora, "A cobweb model with gradient adjustment mechanism: nonlinear dynamics and multistability," *Journal of Difference Equations and Applications*, vol. 24, no. 2, pp. 1–18, 2018.

[3] R. F. AbuAlRub, "Nursing shortage in Jordan: what is the solution?," *Journal of Professional Nursing*, vol. 23, no. 2, pp. 117–120, 2007.

[4] A. Naimzada and N. Pecora, "Memory, market stability and attractors coexistence in a nonlinear cobweb model," *Journal of Difference Equations and Applications*, vol. 22, no. 6, pp. 766–779, 2016.

[5] R. Dieci and F. Westerhoff, "Stability analysis of a cobweb model with market interactions," *Applied Mathematics and Computation*, vol. 215, no. 6, pp. 2011–2023, 2009.

[6] R. Thaler, *The Winner's Curse: Paradoxes and Anomalies of Economic Life*, Simon and Schuster Press, New York, USA, 2012.

[7] W. A. Brock and C. H. Hommes, "A rational route to randomness," *Econometrica*, vol. 65, no. 5, pp. 1059–1095, 1997.

[8] W. A. Branch and B. McGough, "Replicator dynamics in a Cobweb model with rationally heterogeneous expectations," *Journal of Economic Behavior & Organization*, vol. 65, no. 2, pp. 224–244, 2008.

[9] S. N. Elaydi, *An Introduction to Difference Equations*, Springer-Verlag New York Inc, Secaucus, NJ, USA, 1996.

[10] M. F. EL-Wakeel, S. S. Askar, and N. A. Alkhunayfir, "Toward investigation of the complex behavior of a monopoly game," *Journal of Computational and Theoretical Nanoscience*, vol. 13, no. 11, pp. 8552–8559, 2016.

[11] E. I. Jury and M. Mansour, "Stability conditions for a class of delay differential systems," *Internation Journal of Control*, vol. 35, p. 6899699, 1982.

[12] M. S. Shabbir, Q. Din, K. Ahmad, A. Tassaddiq, A. H. Soori, and M. A. Khan, "Stability, bifurcation, and chaos control of a novel discrete-time model involving Allee effect and cannibalism," *Advances in Difference Equations*, vol. 2020, no. 1, p. 379, 2020.

[13] S. S. Zhou, H. Jahanshahi, Q. Din et al., "Discrete-time macroeconomic system: bifurcation analysis and synchronization using fuzzy-based activation feedback control," *Chaos, Solitons & Fractals*, vol. 142, Article ID 110378, 2021.

[14] Q. Din and K. Haider, "Discretization, bifurcation analysis and chaos control for Schnakenberg model," *Journal of Mathematical Chemistry*, vol. 58, no. 8, pp. 1615–1649, 2020.

[15] B. L. Cerboni and A. K. Naimzada, "An oligopoly model with best response and imitation rules," *Applied Mathematics and Computation*, vol. 336, pp. 193–205, 2018.

[16] A. Agliari, A. K. Naimzada, and N. Pecora, "Nonlinear dynamics of a Cournot duopoly game with differentiated products," *Applied Mathematics and Computation*, vol. 281, pp. 1–15, 2016.

[17] H. Bao, Z. Hua, N. Wang, L. Zhu, M. Chen, and B. Bao, "Initials-boosted coexisting chaos in a 2-D sine map and its hardware implementation," *IEEE Transactions on Industrial Informatics*, vol. 17, no. 2, pp. 1132–1140, 2021.

[18] H. Li, Z. Hua, H. Bao, L. Zhu, M. Chen, and B. Bao, "Two-dimensional memristive hyperchaotic maps and application in secure communication," *IEEE Transactions on Industrial Electronics*, p. 1, 2021.

[19] B. C. Bao, H. Z. Li, L. Zhu, X. Zhang, and M. Chen, "Initial-switched boosting bifurcations in 2D hyperchaotic map," *Chaos: An Interdisciplinary Journal of Nonlinear Science*, vol. 30, no. 3, p. 033107, 2020.

[20] W. C. Wheaton, "Real estate "cycles": some fundamentals," *Real Estate Economics*, vol. 27, no. 2, pp. 209–230, 1999.

[21] W. M. Simmons, *An Economic Study of the US Potato Industry*, US Dept. of Agriculture, Economic Research Service, Economic and Statistical Analysis Division, Washington, DC, USA, 1962.

[22] L. Lundberg, E. Jonson, K. Lindgren, D. Bryngelsson, and V. Verendel, "A cobweb model of land-use competition between food and bioenergy crops," *Journal of Economic Dynamics and Control*, vol. 53, pp. 1–14, 2015.

[23] R. Manning, "Stability of cobwebs," *Journal of Economic Behavior and Organization*, vol. 24, no. 3, pp. 315–335, 1970.

[24] M. Nerlove, "Adaptive expectations and cobweb phenomena," *The Quarterly Journal of Economics*, vol. 72, no. 2, pp. 227–240, 1958.

[25] C. Chiarella, "The cobweb model," *Economic Modelling*, vol. 5, no. 4, pp. 377–384, 1988.

[26] C. H. Hommes, "Dynamics of the cobweb model with adaptive expectations and nonlinear supply and demand," *Journal of Economic Behavior & Organization*, vol. 24, no. 3, pp. 315–335, 1994.

[27] C. H. Hommes, "Adaptive learning and roads to chaos," *Economics Letters*, vol. 36, no. 2, pp. 127–132, 1991.

[28] C. Engel and H. Hamann, "The hog cycle of law professors: an econometric time series analysis of the entry-level job market in legal Academia," *PLoS One*, vol. 11, no. 12, Article ID e0159815, 2016.

[29] S. S. Askar and A. Al-Khedhairi, "Analysis of nonlinear duopoly games with product differentiation: stability, global dynamics, and control," *Discrete Dynamics in Nature and Society*, vol. 2017, Article ID 2585708, 13 pages, 2017.

[30] E. Ahmed, A. S. Hegazi, M. F. Elettreby, and S. S. Askar, "On multi-team games," *Physica A: Statistical Mechanics and Its Applications*, vol. 369, no. 2, pp. 809–816, 2006.

[31] S. S. Askar, "Tripoly Stackelberg game model: one leader versus two followers," *Applied Mathematics and Computation*, vol. 328, pp. 301–311, 2018.

[32] S. S. Askar and K. Alnowibet, "Cooperation versus noncooperation: Cournot duopolistic game based on delay and time-dependent parameters," *Chaos, Solitons & Fractals*, vol. 91, pp. 580–584, 2016.

[33] E. Ahmed and M. F. Elettreby, "Controls of the complex dynamics of a multi-market Cournot model," *Economic Modelling*, vol. 37, pp. 251–254, 2014.

[34] S. S. Askar and M. Abouhawwash, "Quantity and price competition in a differentiated triopoly: static and dynamic investigations," *Nonlinear Dynamics*, vol. 91, no. 3, pp. 1963–1975, 2018.

[35] F. Cavalli, A. Naimzada, and F. Tramontana, "Nonlinear dynamics and global analysis of a heterogeneous Cournot duopoly with a local monopolistic approach versus a gradient rule with endogenous reactivity," *Communications in Nonlinear Science and Numerical Simulation*, vol. 23, no. 1-3, pp. 245–262, 2015.

[36] S. S. Askar and A. Al-khedhairi, "Dynamic investigations in a duopoly game with price competition based on relative profit and profit maximization," *Journal of Computational and Applied Mathematics*, vol. 367, Article ID 112464, 2020.

[37] A. A. Elsadany, "Dynamics of a Cournot duopoly game with bounded rationality based on relative profit maximization," *Applied Mathematics and Computation*, vol. 294, pp. 253–263, 2017.

[38] J. Ma, L. Sun, S. Hou, and X. Zhan, "Complexity study on the Cournot-Bertrand mixed duopoly game model with market share preference," *Chaos: An Interdisciplinary Journal of Nonlinear Science*, vol. 28, no. 2, pp. 23101–23110, 2018.